

DISSERTATION

Qualitative and Quantitative Comparisons between Spar and Semi-Submersible Platforms

Matthew Guan Zhen Hwa

15332

Submitted in partial fulfillment of the requirements for the

Degree of Study (Hons)

Civil Engineering

FYP II Semester 8 and Year 4

Universiti Teknologi PETRONAS

Bandar Seri Iskandar

31750 Tronoh

Perak Darul Ridzuan

CERTIFICATION OF APPROVAL

Qualitative and Quantitative Comparisons between Spar and Semi-Submersible Platforms

by

Matthew Guan Zhen Hwa

15332

Submitted in partial fulfillment of the requirements for the

Degree of Study (Hons)

Civil Engineering

Approved by

UNIVERSITI TEKNOLOGI PETRONAS
TRONOH, PERAK

December 2014

CERTIFICATION OF ORIGINALITY

I hereby certify that I am responsible for the work submitted in this project, and that the original work is my own, excluding those as specified in the references and acknowledgements. The original work contained herein have not been undertaken or carried out by unspecified sources of persons.

MATTHEW

GUAN

ZHEN

HWA

ABSTRACT

Spars and semisubmersibles are two floating platforms commonly used in offshore deepwater exploration and production. However, currently lack of studies are available to comparatively evaluate the two platforms under similar cost range. This study compares the hydrodynamic motions of a truss spar and a semisubmersible under similar cost and wave environment. The platforms were numerically modelled using the radiation/diffraction software HydroSTAR. The response amplitude operators (RAO) were obtained for surge, heave and pitch respectively. The findings indicate the responses for the truss spar are generally lower than the semisubmersible, with the exception for the peak heave and pitch RAO. At 1000 m, the percentage difference of the peak surge RAO for spar and semisubmersible is 0.005%; heave RAO for semisubmersible is 34% of the spar's value; and pitch RAO for semisubmersible is 79% of the spar's value. Additionally, the semisubmersible achieved its peak RAO at a higher frequency for the heave and pitch. The findings proved that overall the spar's dynamic responses are better for the majority of wave frequencies.

ACKNOWLEDGEMENTS

The author would like to dedicate this section to express his gratitude to the various parties and individuals who have contributed to realise this research.

First, I would like to thank my supervisor Dr Montasir for his patient guidance and effort in overseeing my work. Also to the members of the Civil Engineering Department in UTP: Dr Ng, Mr Amal and Mr Anurag who shared their knowledge and experience, as well as other members who have assisted me in work. Without their guidance, this project would not have been completed.

Next, I would like to thank my parents and family who have continually supported me throughout my period of study, providing me the daily necessities to enable and ease my time during this period.

Also, I would like to express my gratitude to my support group as well as others who have indirectly supported me in this study, consequently providing the intrinsic motivation to complete the project.

Last but not least, I would to thank God Almighty in His guidance and strength to overcome the many challenges faced during this period in completing the report.

TABLE OF CONTENTS

ABSTRACT	i
ACKNOWLEDGEMENTS	ii
LIST OF FIGURES	iv
LIST OF TABLES	v
ABBREVIATIONS	vi
CHAPTER 1: INTRODUCTION	1
1.1 Problem Statement	3
1.2 Objective of Study	3
1.3 Scope of Study	4
CHAPTER 2: LITERATURE REVIEW	5
2.1 Behaviour of Spars	5
2.2 Behaviour of Semisubmersibles	6
2.3 Comparing Spars and Semisubmersibles	8
2.4 Conclusion	9
CHAPTER 3: METHODOLOGY	10
3.1 Concept/Theory	10
3.2 Platform Configuration	13
3.3 HydroSTAR Numerical Modelling	16
3.4 Project Timeline	19
CHAPTER 4: RESULTS AND DISCUSSION	20
CHAPTER 5: CONCLUSION AND RECOMMENDATION	28
REFERENCES	29
APPENDICES	31

LIST OF FIGURES

Figure 1.1: Truss spar platform

Figure 1.2: Semisubmersible platform

Figure 3.1: Schematic diagram of a progressive wave train

Figure 3.2: AUTOCAD model of semisubmersible

Figure 3.3: AUTOCAD model of spar

Figure 3.4: Sample .HST file

Figure 3.5: Methodology process

Figure 4.1: Semisubmersible model

Figure 4.2: Spar model

Figure 4.3: Comparison of surge RAO

Figure 4.4: Comparison of heave RAO

Figure 4.5: Comparison of pitch RAO

Figure 4.6: Spar surge RAO

Figure 4.7: Spar heave RAO

Figure 4.8: Spar pitch RAO

Figure 4.9: Semisubmersible surge RAO

Figure 4.10: Semisubmersible heave RAO

Figure 4.11: Semisubmersible pitch RAO

LIST OF TABLES

Table 4.1: Semisubmersible configuration

Table 4.2: Spar configuration

ABBREVIATIONS

CB: Centre of Buoyancy

CG: Centre of Gravity

DOF: Degree-of-freedom

FPSO: Floating Production Storage Offloading

RAO: Response Amplitude Operator

SCR: Steel Catenary Riser

TLP: Tension Leg Platform

CHAPTER 1: INTRODUCTION

The demand for oil and gas is steadily rising. As reserves in onshore and shallow waters become scarce, explorers can either opt to seek new fields, or move into deeper waters. In recent years, the trend of major oil and gas companies gravitates to deep and ultra-deep water fields; as such investment in this area continues to increase (Latham, 2002). Various structures were developed in order to operate under the significantly more challenging deepwater environments. Structures must be considered for their engineering performances as well as cost. Floating structures become a more viable option as fixed platforms become increasingly expensive and difficult to install in deeper waters. These structures often experience severe joint action from waves, current and wind due to harsh weather. As such, it is important to consider the structures' ability to resist environmental loads to accommodate the volatile environment in deepwater regions. This does not only affect the platform safety but also the total cost in manufacturing the platform. Two floating platforms considered in deep and ultra-deepwater environments are spars and semisubmersibles. Both platforms, each with their own distinct structural designs are considered for their performance in deepwater environments.

In 1975, the first floating production system, a converted semi-submersible was installed on Argyle field in the North Sea. Since then, other floating platforms were installed at various fields around the world. In 2002, a total 383 floating systems were recorded (Abbas, 2011). By 2011, more than 120 semisubmersibles and 17 spars are in operation (Li et al. 2011); the number is expected to increase throughout the years.

A semi-submersible is a multi-column structure housing a large deck. These columns are interconnected at the bottom with horizontal pontoons, which provide buoyancy for the structure. Early semi-submersibles are designed with diagonal cross-bracing to withstand prying and racking loads from the waves. The newer generation semi-submersibles generally adopt a shape of a square with four columns interconnected by a box or cylinder shaped pontoons (Chakrabarti, 2005). The diagonal bracing previously present in the early generation semi-submersibles are usually eliminated to simplify the construction process. A semi-submersible's stability is mainly

dependent on the water plane area and metacentric height, as its centre of gravity (CG) is above its centre of buoyancy (CB). This is accomplished by spreading the platform over a large water plane area; doing so increases the natural period of the structure proportionally (Hammett, 1983). Roll, pitch and heave motions are also reduced as a result. Semisubmersibles typically have their natural periods outside of the maximum wave periods. They generally only support wet tree drilling, although recent developments made it possible that allow a semisubmersible that supports dry tree drilling as well. Semisubmersibles are towed to the site or may have their own self-propulsion unit; the latter is also used for station keeping. The platforms are also relatively low in cost compared to other deepwater platforms, especially for a converted unit.

An alternative to a semi-submersible, a spar consists of a deep draft vertical hull designed to support drilling and production operations. There are three types of spars: the classic spar, truss spar and cell spar. In 2009, a total of 17 spars are in operation: three classic spars, 13 truss spars and one cell spar (Sablok & Barras, 2009). All spars are operating in the Gulf of Mexico except the Kikeh truss spar which is deployed in Sabah, Malaysia. The classic spar composes of a single large circular cylinder with a deep draft. The truss spar substitutes the large cylindrical midsection with a truss-type section. The cell spar utilizes of a number of relatively small diameter cylinders (cells) attached symmetrically, compared to a single large diameter of a classic spar (Sablok & Barras, 2009). A spar's the upper section consists of a hard tank which provides the buoyancy, while the lower section houses the soft tank which functions as a fixed ballast. The platforms achieve a high stability due to their CG being lower than their CB. This is made possible by the heavy ballast at the keel. This characteristic enables spars to display low motion response characteristics in response to environmental loads. Spars support dry or wet tree drilling, and are towed to site via barges and tugboats.



Figure 1.1: Truss spar platform

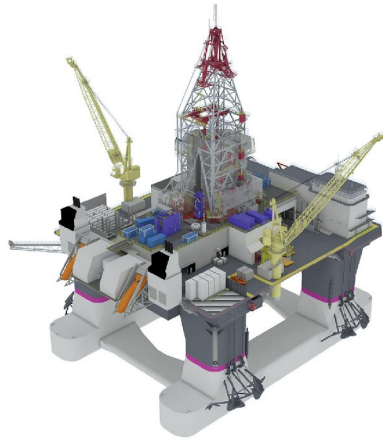


Figure 1.2: Semisubmersible platform

1.1 Problem Statement

Pursuit is continuously ongoing to develop new innovative designs in order to minimize offshore dynamic motions, and therefore the cost of producing the platforms. Much can be discovered by comparing the various types of floating platforms available, and exploring the characteristics of each of these platforms. This is significant in order to achieve optimum design under a given environment with minimum investment cost. While much research has been carried out concerning the dynamic characteristics of the two platforms, less study was attempted to compare their characteristics under similar environment and cost. Hence, it is difficult to fairly assess the platforms' behaviors, in order to integrate their characteristics to produce a new innovative design that minimizes the dynamic motions at sea.

1.2 Objective of Study

The primary objective of this research is to compare the dynamic motions (i.e. the response amplitude operators, RAO) of the spar and semi-submersible platforms under similar cost and operating environments, with cost being equated to the weight of steel used in fabricating the platform. Additionally, the responses of the platforms under varying water depth are analysed as a secondary objective. The analysis is carried out using the radiation/diffraction software HydroSTAR.

1.3 Scope of Study

This study is carried out under the following constraints:

1. Only a truss spar and semi-submersible platform is considered.
2. The hydrodynamic motions analysed considers only the wave parameter.
3. Waves are taken as regular and unidirectional.
4. Responses are analysed in three degrees of freedom: surge, heave and pitch.
5. Mooring line stiffness is configured the same for both platforms.

CHAPTER 2: LITERATURE REVIEW

2.1 Behaviour of Spars

In 2012, Kurian et al. studied the dynamic motions of a truss spar under wave, wind and current forces. It was found that, while waves were the main contributors to the motion amplitude, current and wind forces, while having negligible impact on the amplitude, significantly increased the surge mean offset of the structure.

Another research was conducted by Chen in 2002, concerning the damping effects on mooring lines on low frequency drift motions of a JIP spar. He discovered that the dynamic coupling effects between the spar and mooring system were significant, especially moving into deeper waters. The mooring line significantly lowered the slow drift surge, and this reduction increased with increasing water depth. The dynamic forces of the mooring lines were also found to have minimal impact on the wave frequency motion of the spar, as the mass of the mooring lines is small compared to the mass of the spar and wave loads. However, oscillation in the mooring lines resulted in large tensions of the wave frequency range.

Liu et al. (2010) analysed the parameters of number, spacing and thickness of heave plates, and its effect on the motion responses of truss spars. By increasing the number of heave plates, they discovered that the heave excitation force significantly decreased while the added mass increased; however too many heave plates resulted in inefficient reduction in the motion response. In addition, optimum heave response is obtained when the vertical spacing between the heave plates is equal to the side length of the square heave plate; this configuration achieves maximum added mass as well. It was also observed that, by increasing the thickness of the heave plate, this will result in the decrease of the metacentric height. However, it was noted that the thickness of the heave plates does not significantly affect the heave and pitch response amplitude operators (RAO).

2.2 Behaviour of Semisubmersibles

Abbas (2011) conducted a comprehensive study on the non-linear interactions of a moored semisubmersible. He found that the heave response was influenced by water depth at low frequency. Furthermore at a given frequency, the drift force coefficient reduced as the wave amplitude increased; this reduction percentage increased with increasing amplitude.

In his analysis between the mooring and seabed interactions, the dynamic tensions in the mooring line was directly proportional to the wave motion frequency. When the mooring line was attached to the spring buoy, the rate at which the dynamic tension increases with respect to the wave motion was generally lower, especially at higher frequencies. In addition, the tension decreased as the soil stiffness increases. Furthermore, the writer's investigations showed that the higher the soil damping, the lower the mooring line tensions. For very stiff soils, low frequency wave motions allowed for reduced mooring line tension; this effect reverses at high frequencies due to large impact. The soil damping dissipated the impact due to dynamic forces of the mooring system, resulting in reduced mooring line tensions especially at high frequency wave motions. Because of the direction nature of soil reactive forces, tensions in the vertical component are more influenced by soil damping compared to the horizontal components.

On the design parameters of moored semisubmersibles, Abbas found that, for multicomponent mooring lines, the horizontal restoring force is directly proportional to the pretension and the unit weight, while being inversely proportional to the pretension angle for positive excursions. However, the restoring force becomes independent of the mooring length and clump weight after attaining a certain value of tension. For negative excursions, the pretension angle and axial stiffness have insignificant effect on the restoring forces. Prior to lifting off the clump weight, the vertical restoring force is proportional to the pretension and pretension angle; the restoring force is proportional to the clump unit weight after lifting it off. The force-excursion relationship is also proportional for low range excursions prior to lifting off the clump weight. Additionally the hull cross-sectional height was observed as the dominant effect on the platform's sea-keeping performance. For a small increase in draft, the hydrodynamic loads increases more than the

increase in added mass; while for a large increase in draft, the added mass increases more rapidly than the increase in hydrodynamic load, resulting in the decrease in system response.

During a study to compare the effects of semisubmersible vessel motions using fully coupled approach (considering the dynamic interactions of drag and inertia) and quasi-static approach (which ignores the dynamic interactions), Ye et al. (2003) noted that the primary contributor to the steel catenary riser's (SCR) fatigue damage is the vessel motion of the semisubmersible. The mooring line and riser dynamics have significant impact on the structure's resonant low frequency motions by contributing to the drag damping, thus supporting the findings of Abbas concerning the relationship between the responses with the wave frequency. A separate study carried out by Kurian et al. (2013) also revealed that the response amplitudes develop a similar pattern of maximum amplitude at the low frequency range, gradually reducing as the wave frequency increased. Ye et al. noted however, that the mooring line and riser dynamics do not affect its non-resonant wave frequency motions. Furthermore, the semisubmersible's low frequency motions have moderate effects on the SCR's fatigue damage at the touch down point due to spreading of damage; however, significant increase in fatigue damage is experienced near the hang-off.

2.3 Comparing Spars and Semisubmersibles

In 2011, Li et al. compared the hydrodynamic behaviours of a typical semisubmersible, TLP and truss spar in the South China Sea environment, of which only the semisubmersible and spar will be discussed here. Comparing the surge wave frequency responses, the trend of the two platforms were almost identical to each other, with relatively low deviation in the values. On the other hand, the heave RAO for the semisubmersible in the wave-frequency range is larger than the spar's; however, it was smaller in the low-frequency region. Furthermore, the heave RAO of the spar is observed to vary smoothly with the frequency. This is due to the vertical motions suppressed due to the deep draft and heave plate. Concerning the pitch, the spar response is generally significantly higher than the semisubmersible due to the large rotational moments generated from the wind and current, and the large moment arm which is induced by the low CG. In addition, the natural period of the spar is higher than that of the semisubmersible. Moreover, the heave and pitch RAO for both platforms have a well-defined peak, with the semisubmersible achieving its peak RAO at a later frequency compared to the spar.

In another study, Ng in 2010 assessed the responses of a truss spar and semisubmersible during a research to compare numerical analysis with actual physical model testing. The findings showed somewhat similar patterns as with Li et al. for the responses of surge, heave and pitch; however, the semisubmersible responses were found to have a less well defined peak in the heave and pitch compared to the spar. Furthermore, it was observed that for the pitch, Ng recorded a significantly higher RAO for the spar (up to five times) within the frequency range of 0.1 to 0.3 Hz. The semisubmersible RAO was observed to increase the lower the frequency, while the spar which achieves its peak at a higher frequency than the semisubmersible, contrary to the findings of Li et al. who observed that the semisubmersible achieved a high peak at a higher frequency than its spar counterpart, with the variance in RAO at a smaller degree. These differences could be due to the different geometrical shape of the semisubmersible used in the two studies respectively, in addition to the wind and current loads not considered in Ng's research.

2.4 Conclusion

From the various studies it can be seen that much research has been carried out to determine the hydrodynamic behaviours of spar and semisubmersible platforms. The studies, while distinct and unique in the parameters analysed complemented each other, building on fundamental concepts and theoretical knowledge, aided by numerical computation software. It can be seen that the structures are governed by similar parameters such as the draft, weight and metacentric height.

However, the current studies do not provide sufficient comparison of the performance between the two offshore platforms. While the study conducted by Li et al. attempted to adequately compare between the platforms, it assessed or scaled the structures under typical design configurations; and did not evaluate the platforms under similar costing and mooring configurations. Furthermore, in Li et al. the researchers focused in the environment of the South China Sea, which may not be applicable elsewhere. On the other hand, Ng's research focused on assessing the Morison and diffraction theories against physical model tests, and does not explicitly compare the two platforms.

CHAPTER 3: METHODOLOGY

3.1 Concept/Theory

Various theories may be employed for describing a wave. Some common wave theories include the first order Linear Airy Wave theory, and other higher order wave theories such as Stokes Wave theory for finite amplitude waves, and Cnoidal Wave theory for regular long waves of finite amplitude in shallow water. The Linear Airy Wave theory is widely used due to its simplicity, and is used in the HydroSTAR computation. This theory, also identified as a small amplitude wave theory, assumes that the wave height is small compared to its wave length and water depth. Additionally, the theory assumes a sinusoidal wave pattern, with the crest and trough being of equal amplitude. The Airy Wave Theory is proven to provide a good estimate for deep water wave calculation ($d/L > 0.5$).

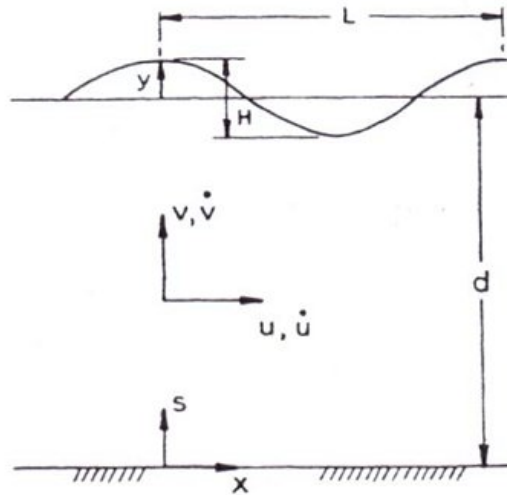


Figure 3.1: Schematic diagram of a progressive wave train

The basic equations are given in the following. The wave number (k) and wave frequency (ω) are given in Equation (1) and (2) respectively, T being the wave period. Multiplying k with the distance x and ω with time t will result in the phase angle θ shown in Equation (3).

$$k = 2\pi/L \quad (1)$$

$$\omega = 2\pi/T \quad (2)$$

$$\theta = kx - \omega t \quad (3)$$

For the Airy Wave Theory, the velocity potential is given as in Equation (4). Differentiating ϕ in terms of x and y will yield the horizontal particle velocity (u) and vertical particle velocity (v) respectively (Equation 5 and 6). Further differentiating Equation (5) and (6) will result in the horizontal acceleration \dot{u} (Equation 7) and vertical acceleration \dot{v} (Equation 8) respectively. On the other hand, integrating Equation (5) and (6) will obtain their displacements for the horizontal (ξ) and vertical (η) direction respectively.

$$\phi = \frac{\pi H \cosh ks}{kT \sinh kd} \sin \theta \quad (4)$$

$$u = \frac{\partial \phi}{\partial x} = \frac{\pi H \cosh ks}{T \sinh kd} \cos \theta \quad (5)$$

$$v = \frac{\partial \phi}{\partial y} = \frac{\pi H \sinh ks}{T \sinh kd} \sin \theta \quad (6)$$

$$\dot{u} = \frac{\partial u}{\partial t} = \frac{2\pi^2 H \cosh ks}{T^2 \sinh kd} \sin \theta \quad (7)$$

$$\dot{v} = \frac{\partial v}{\partial t} = -\frac{2\pi^2 H \sinh ks}{T^2 \sinh kd} \cos \theta \quad (8)$$

$$\xi = -\frac{H \cosh ks}{2 \sinh kd} \sin \theta \quad (9)$$

$$\eta = \frac{H \sinh ks}{2 \sinh kd} \cos \theta \quad (10)$$

In computing the dynamic responses, three theories may be used. The first is the Morison's theory, which considers the wave force to be composed of two components, inertia and drag,

linearly added together. This theory is applicable for platforms experiencing significant drag force, as is commonly the case for small structures relative to the water wave length.

The second theory is the Froude-Krylov theory. Unlike the Morison's equation, this theory is suitable for small structures whose drag force is insignificant compared to its inertia force. The force is determined by the pressure area method generated by undisturbed waves acting on the surface of the structure.

The final theory that can be used to predict the dynamic responses is the diffraction theory. This theory is used when the presence of the structure will significantly affect the surrounding wave field; hence, the wave diffraction effects from the surface of the structure should be considered. This theory is applicable for large structures comparable to the water wave length.

Of the three theories, Morison's theory is generally favoured due to its simplicity in calculation, while the diffraction theory is complex and require costly commercial software. According to Kurian et al. (2012), this practice is justifiable when the ratio of size to wave length falls in the Morison regime for waves of large frequency ($D/L < 0.2$). However, when the value falls outside the regime, Morison's equation can no longer be applicable, and the diffraction theory is used.

In order to verify the suitability of Morison's theory, Ng conducted a study in 2010 to compare the Morison and diffraction theories against a physical model testing. It was revealed that, for a spar and semisubmersible, the results for the diffraction theory was significantly closer to the actual model test compared to the Morison equation. Hence, the use of the HydroSTAR software, which computes the responses using the diffraction/radiation theory, is justified in this study.

In the analysis, the spar and semisubmersible can be approximated as under three degrees-of-freedom (DOF) of surge, pitch and heave. This is because the spar can be considered as a rigid

cylindrical body; as such the wave forces act equally in all directions. Similarly, a semisubmersible is approximated using the 3 DOF, as due to the chosen symmetrical design.

3.2 Platform Configuration

The first stage requires the establishment of the spar and semisubmersible dimensions. The Tahiti spar, referenced in D'Souza et al. (2014) was preliminarily used as the rough guide in setting the dimensions and weight of the to-be modelled spar. For the semisubmersible, the Atlantis platform from the same reference was used.

The dimensions and weight was then scaled to balance the two platforms. The platforms had to be balanced in order for their weights to be comparatively equal. The weight of the platforms were designed such that the volume – and thus mass – of steel used are relatively equal. In addition, the draft of the structures should be designed within acceptable range as during a platform operation.

A spreadsheet was developed in order to achieve the above sub-objective. It also included calculation for the CG as well as the radius of gyration, which are part of the required input for HydroSTAR. As previously noted, the CG for a spar is below its CB, and vice versa for a semisubmersible. The draft/CG value was manipulated by

1. Modifying the hull diameter of the spar
2. Adjusting the height of the hard tank and soft tank
3. Modifying the size and height of the semisubmersible column
4. Modifying the total square area covered by the semisubmersible
5. Adjusting the volume/weight distribution of the platforms

As the CB is calculated by HydroSTAR, only the CG was computed during configuration.

The equation for CG is given as

$$\bar{x} = \frac{\sum_{j=1}^N m_n x_n}{\sum_{j=1}^N m_n} \quad (11)$$

Where m_n = mass of steel at section n, and x_n = distance of CG of section n from reference point.

For the radius of gyration (k), the equation is expressed as

$$k = \sqrt{\frac{I}{M}} \quad (12)$$

Where I = total moment of inertia, and M = total mass.

A platform is composed of different geometries. Consequently, the moment of inertia differs for each shape, as well as the location of the body's centroid in respect to the rotary axis. The mass moment of inertia, in kgm^2 is calculated using the following equations:

1. Rectangular blocks

$$I_x = \frac{1}{12}m(y^2 + z^2) + me^2 \quad (13)$$

$$I_y = \frac{1}{12}m(x^2 + z^2) + me^2 \quad (14)$$

$$I_z = \frac{1}{12}m(x^2 + y^2) + me^2 \quad (15)$$

Where m = mass of the plate, and x , y and z are the length of the plate in the respective direction, and e = eccentricity.

2. Cylinder

$$I_z = \frac{1}{2}m(r_2^2 + r_1^2) + me^2 \quad (16)$$

$$I_x = I_y = \frac{1}{12}m[3 + (r_2^2 + r_1^2) + h^2] + me^2 \quad (17)$$

Where r_1^2 = inner radius, r_2^2 = outer radius, and h = height of cylinder.

During configuration, a model was also generated using AUTOCAD software for the spar and semisubmersible respectively, applying the established dimensions. The models serve as the initial visual reference, as HydroSTAR's model mesh can only be made through text input. Used in conjunction with the aforementioned spreadsheet, The AUTOCAD models greatly assisted in the design in various ways, as listed below:

1. Models and its segments can be easily generated, modified or hidden as necessary
2. Models are displayed real-time and can be rotated
3. World coordinates can be provided at each point or line of the model
4. Nodes and panels can be labeled for ease of reference
5. Properties/dimensions for a line/object can be easily displayed

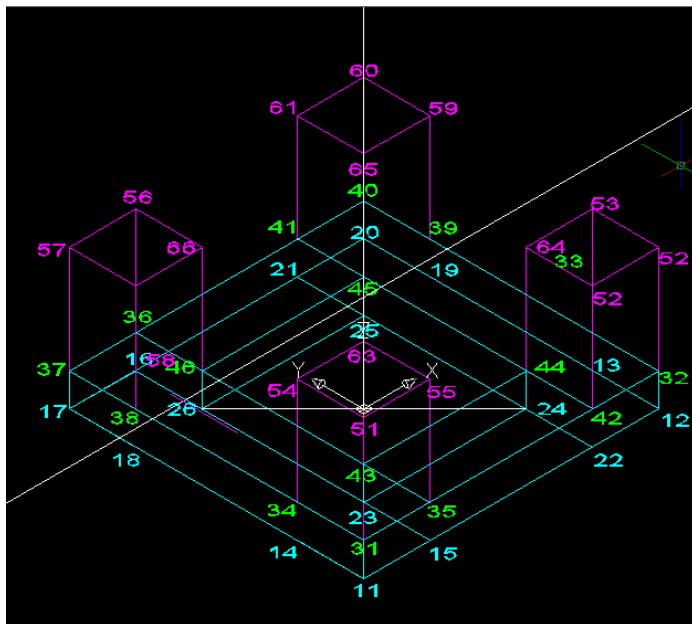


Figure 3.2: AUTOCAD model of semisubmersible spar

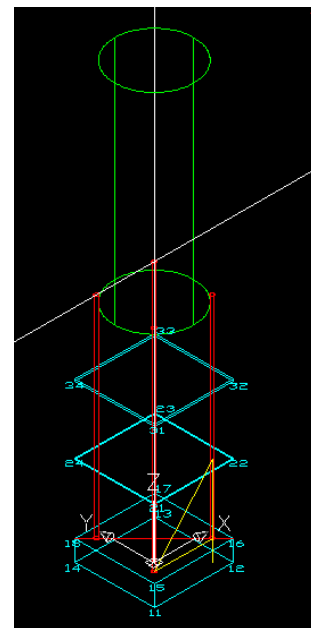


Figure 3.3: AUTOCAD model of semisubmersible platform

Additionally, the stiffness of the platforms needed to be considered, and were represented in matrix form for surge, heave and pitch. The total stiffness is composed of the mooring and hydrostatic stiffness.

For the spar, the total stiffness is expressed as

$$K = \begin{bmatrix} k_x & 0 & -k_x\delta \\ 0 & \rho g A_s & 0 \\ -k_x\delta & 0 & -k_x\delta^2 + \rho A_s D (y_{CG} - y_{CB}) \end{bmatrix} \quad (18)$$

Where k_x = mooring line stiffness, δ = distance from CG to fairleads, ρ = water density, A_s = water plane area and D = spar diameter.

For the semisubmersible, the total stiffness is expressed as

$$K = \begin{bmatrix} k_x & 0 & -k_x\delta \\ 0 & \rho g A_s & \rho g \Delta GM \\ -k_x\delta & 0 & k_x\delta^2 \end{bmatrix} \quad (19)$$

Where Δ = water displacement by volume, GM = metacentric height.

3.3 HydroSTAR Numerical Modelling

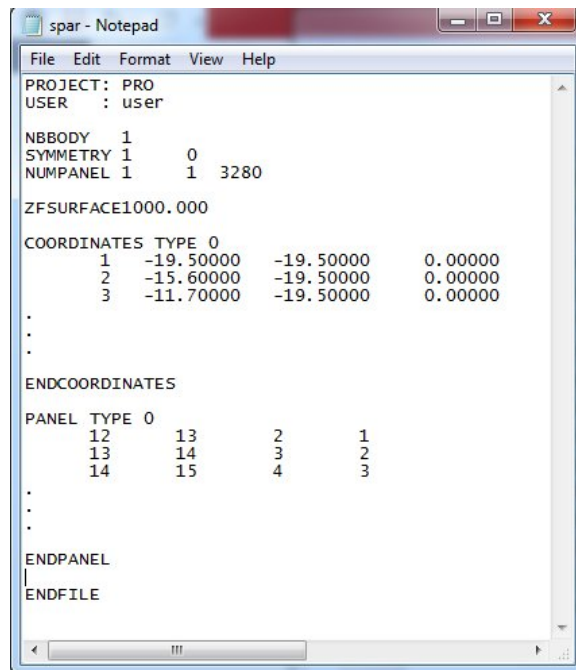
Once the platforms configurations were established, the data was used as input for the HydroSTAR analysis. The steps taken to numerically model the platforms are described below.

First, the mesh was generated for the HydroSTAR. The software required the input of text strings and characters, created using the default Notepad program. HydroSTAR houses a built-in automatic mesh generator for simple geometrical shapes; however, a truss spar and semisubmersible is a complex structure composing of different geometries, hence the need to provide a custom input.

In HydroSTAR, the platforms are made out of multiple bodies or patches. A patch is formed by connecting four nodes. Each node and its coordinates was defined. For a circle, the centre point, radius, and first and last angles was input. Input for a cylinder include the centre point and radius

for both for both ends, and the first and last angles. In addition, the number of elements that made up each patch was defined. Higher number of elements allows for a more detailed and accurate analysis but also increases computation time. To generate a body, various patches and segments were combined in order to build the mesh.

In the Notepad file, a custom/non-symmetrical body was established. Next, the nodes that were to be used were created. Nodes were grouped according to the portion of the platform in which they would be composing. The patches were then generated with the designated nodes, and the input is saved as .MSH file. Under HydroSTAR, the MSH file was executed. HydroSTAR would then generate a .HST file, as shown in Figure 3.4.



```
File Edit Format View Help
PROJECT: PRO
USER : user

NBBODY 1
SYMMETRY 1 0
Numpanel 1 1 3280

ZFSURFACE1000.000

COORDINATES TYPE 0
 1 -19.50000 -19.50000 0.00000
 2 -15.60000 -19.50000 0.00000
 3 -11.70000 -19.50000 0.00000
.
.
.
ENDCOORDINATES

PANEL TYPE 0
 12 13 2 1
 13 14 3 2
 14 15 4 3
.
.
.
ENDPANEL
ENDFILE
```

Figure 3.4: Sample .HST file

HydroSTAR required the .HST file to be read, which will calculate and establish several properties, such as the CB of the platform. Later, the mesh was checked through the software, to verify the consistency, panel properties, and reveal potential errors of the mesh.

Once the platform mesh was confirmed free from error, the sea parameters was established. This included the wave range, incident wave angle and water depth. The file is saved as a .RDF file. Computation for radiation and diffraction was then started.

The next process was to input the mechanical properties of the platforms. The mass, CG, radius of gyration and stiffness matrix established during configuration was saved as a .MEC file, and executed to compute the platform motions.

Once the mechanical computations were performed, the second order mean drift loads were calculated. Input was defined for near-field, middle-field and far-field formulations. For the middle-field formulation, a control surface had to be defined for the area surrounding the vicinity of the platform. The input was saved as a .DFT file for execution.

The final step is to generate the results. The input file containing required transfer functions, i.e. the RAO was prepared as a .RAO file. The results were then generated in tabular form and represented graphically.

Figure 3.5 summarises the methodology process for the HydroSTAR undertaken in this project.

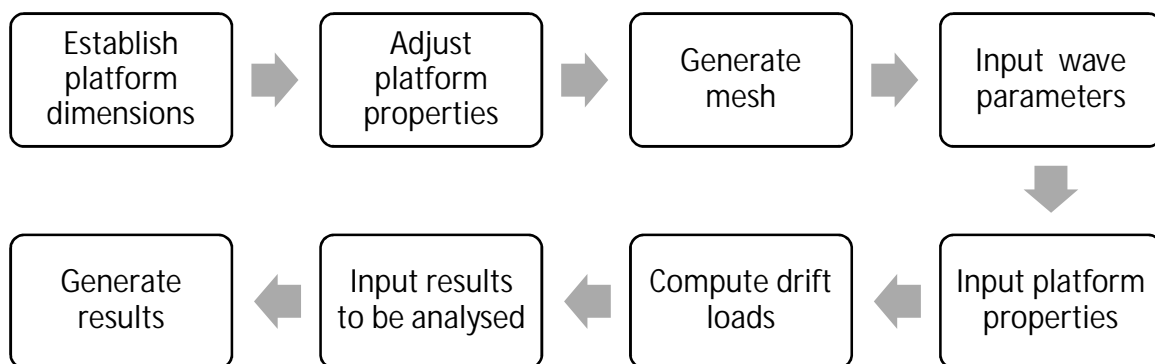


Figure 3.5: Methodology process

3.4 Project Timeline

Activity/week	FYP 1														FYP 2													
	1	2	3	4	5	6	7	8	9	10	11	12	13	14	15	16	17	18	19	20	21	22	23	24	25	26	27	28
Topic Selection	█	█																										
Submission of Topic Selection		█																										
Literature Review			█	█	█	█	█	█	█	█	█	█	█	█														
Submission of Extended Proposal						█																						
Software Familiarisation							█	█	█	█	█	█	█	█														
Proposal Defence									█	█																		
Submission of Interim Draft Report												█																
Submission of Interim Report													█															
Platform Configuration													█	█														
Software Modelling															█	█	█	█	█	█	█							
Software Analysis																					█	█	█					
Reporting																					█	█	█	█	█			
Submission of Progress Report																						█						
Pre-SEDEX																								█				
Submission of Final Draft Report																									█			
Submission of Dissertation (softbound) and Technical Paper																										█		
Viva																											█	
Submission of Project Dissertation (Hard Bound)																												█

Legend:

	Activity period		Milestone
--	-----------------	--	-----------

CHAPTER 4: RESULTS AND DISCUSSION

The general data for the spar and semisubmersible are presented in Table 4.1 and 4.2. The CG is taken with bottom surface of the pontoon/soft tank as 0, while the radius of gyration is obtained using the CG as the reference point. Only the CG in the vertical z-axis is given, as both structures are symmetrical and thus have the CG in the x and y-axis in the centre of the platform.

Item	Unit	Value
Column dimension (L x W x H)	m x m x m	18 x 18 x 29
Column spacing	m	62
Pontoon dimension (W x H)	m x m	18 x 9
Total mass	tonne	60600
Draft	m	23.6
Centre of gravity:	m	18.9
Radius of gyration:	Rxx	31.3
	Ryy	31.3
	Rzz	36.9
Mooring line stiffness	kN	532

Table 4.1: Semisubmersible configuration

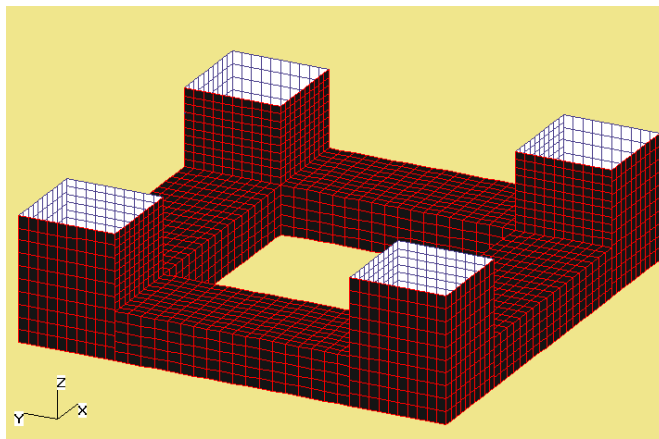
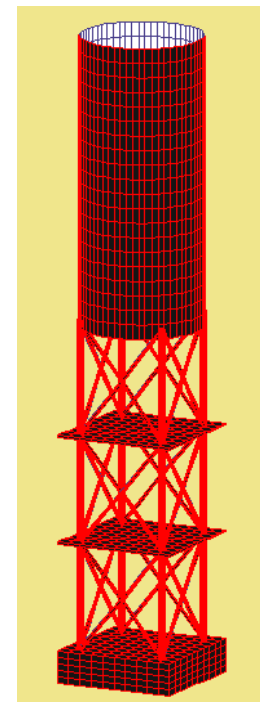


Figure 4.1: Semisubmersible model

Item	Unit	Value
------	------	-------



Hard tank diameter	m	30
Hard tank height	m	80
No. of heave plates	-	2
Heave plate dimension (L x W x H)	m x m x m	30 x 30 x 0.5
Soft tank (L x W x H)	m x m x m	30 x 30 x 8
Vertical truss diameter	m	1.5
Diagonal truss diameter	m	0.8
Hull height	m	166
Total mass	tonne	60600
Draft	m	156.7
Centre of gravity:	m	99.4
Radius of gyration:	Rxx	70.4
	Ryy	70.4
	Rzz	13.7
Mooring line stiffness	kN	532

Table 4.2: Spar configuration

Figure 4.2: Spar model

The responses of the spar and semisubmersible platforms at a depth of 1000 m are obtained and compared as shown in Figures 4.3 to 4.5.

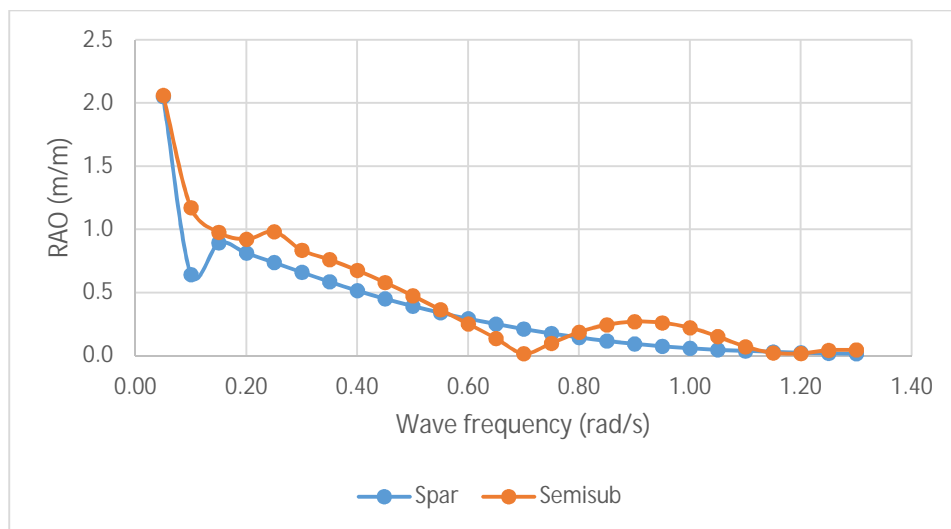


Figure 4.3: Comparison of surge RAO

It is observed that the surge RAO for both platforms are relatively similar, with the spar having slightly lower RAO for the majority of the frequency range. The reason for this is because the

response in the surge direction is for the most part dependent on the mooring stiffness, which had been set the same for both platforms. The maximum surge RAO for spar and semisubmersible is 2.05 m/m and 2.06 m/m respectively – a negligible percentage difference of 0.005% – and are located at lowest observed frequency of 0.05 rad/s.

It was also noted that as the frequency increases, the surge response of the semisubmersible generally dipped until 0.7 rad/s, afterwards experiencing a slight increase up to the 0.9 rad/s frequency before decreasing back. This “valley value” at 0.7 rad/s corresponds to the cancellation period of the platform, which is influenced by the shape of the hull (Li et al., 2011). The trend showed good agreement with the findings by both Ng and Li et al.

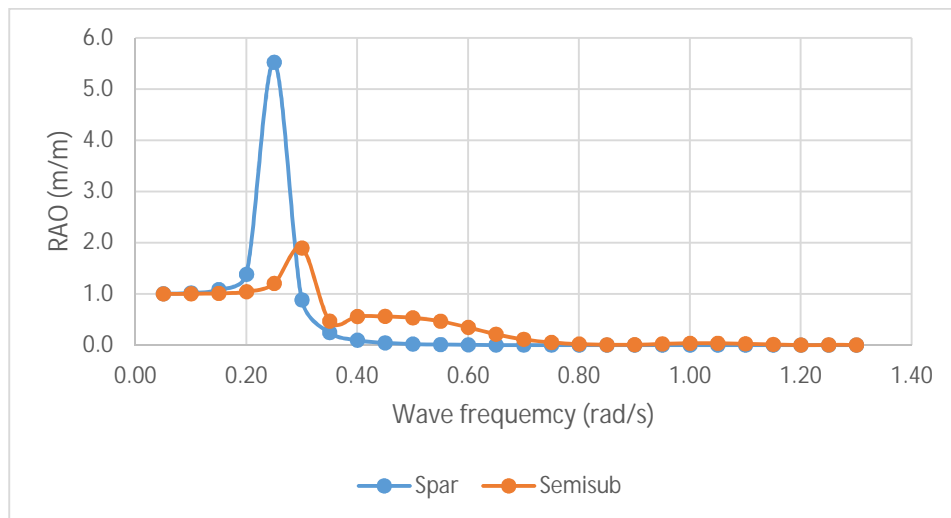


Figure 4.4: Comparison of heave RAO

For the heave response, it is found that the peak RAO for the spar is significantly higher than the semisubmersible, with the semisubmersible RAO at 1.90 m/m, 34% the value of the spar RAO which is at 5.52 m/m. This is because, although the spar has the benefit of a deep draft and heave plates, the water plane area and the heave added mass of the semisubmersible is ultimately larger than the spar. However, notwithstanding the peak, majority of the responses were lower for the spar. Its trend also varies smoother compared to the semisubmersible.

Additionally, it is observed that the spar reaches its peak heave RAO at a slightly lower wave frequency than the semisubmersible. This shows that the natural frequency for the spar is lower than that of the semisubmersible, which can be proven through the natural frequency formula, $f = \sqrt{k/m}$, where k is the stiffness m is the total mass. The equation is applied in conjunction with the stiffness matrix previously developed in the methodology. From this, it is calculated that the natural frequencies are within the peak point locations of the RAO. Again, the findings are observed to be similar to the graphical plot obtained Li et al.; however the trend significantly varied from Ng, whose results indicate that the semisubmersible achieves its peak at a lower frequency than the spar. This could be due to the geometric shape of the semisubmersible, in which Ng adopted a two pontoon eight column design, in contrast to the symmetrical four pontoon four column used in this study.

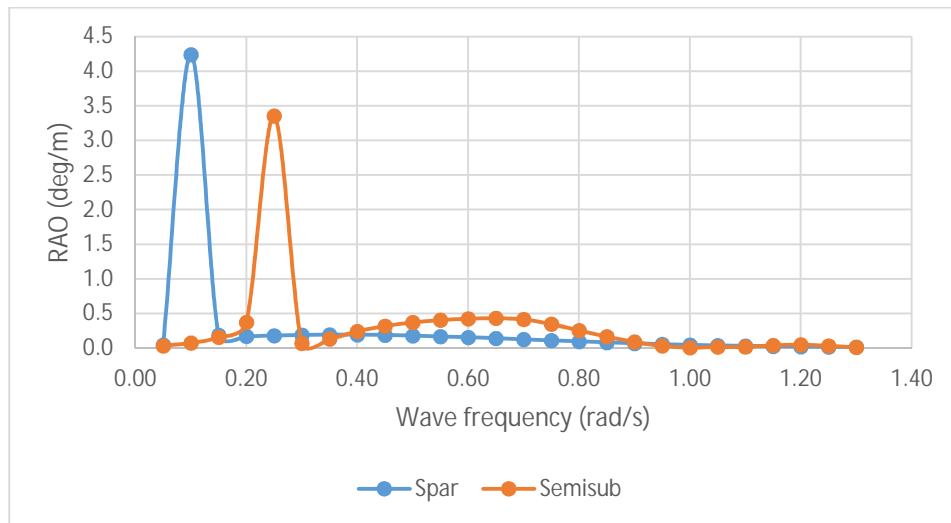


Figure 4.5: Comparison of pitch RAO

Similar to the heave, the peak pitch RAO for the spar is higher than the semisubmersible, achieving 4.24 deg/m while the semisubmersible reaches its peak at 3.35 deg/m – 79% the value of the spar. Here the findings deviate from that of Li et al., whose peak value is higher for the semisubmersible than the spar; however, the obtained values seem to show higher correlation with the results by Ng. This can be due to the semisubmersible covering a large area from one

pontoon to the other, therefore increasing its stability against pitch. After 0.35 rad/s however, it was observed that the semisubmersible RAO increases and maintains above the spar. Additionally, the spar reaches its peak at a lower frequency compared to the semisubmersible, similar to trend observed in the heave direction.

An analysis was also conducted to study the effects of water depth against the dynamic responses. The surge, heave and pitch for the spar is represented in Figures 4.6 to 4.8 respectively; while the surge, heave and pitch for the semisubmersible is shown in Figures 4.9 to 4.11 respectively. Three depths were analysed: at 1000 m, 1500 m and 2000 m.

From the plots, it was observed that for the spar, the surge and pitch showed a slight increase in RAO with decreasing water depth at the low frequency range. Likewise for the semisubmersible, the response increases as the depth decreases, but in the surge direction only. The remaining responses were considered insignificant in affecting the performance of the platforms. In addition, the trends for the plots retained their respective patterns.

The increase in response is due to the platform interaction with the waves and bottom surface of the seabed. At low frequency, the wavelength is significantly large and the effect becomes more pronounced, subsequently affecting the dynamic responses of a platform.

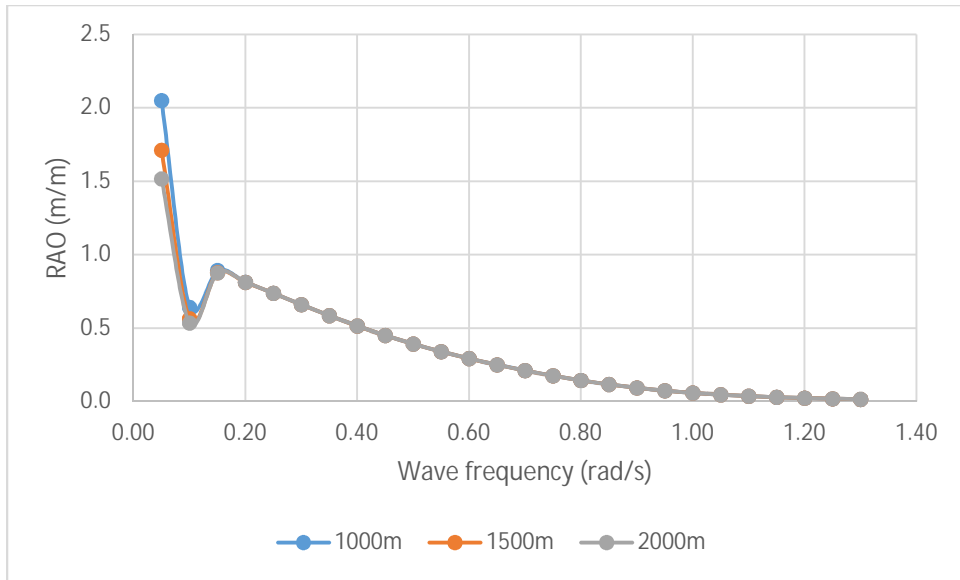


Figure 4.6: Spar surge RAO

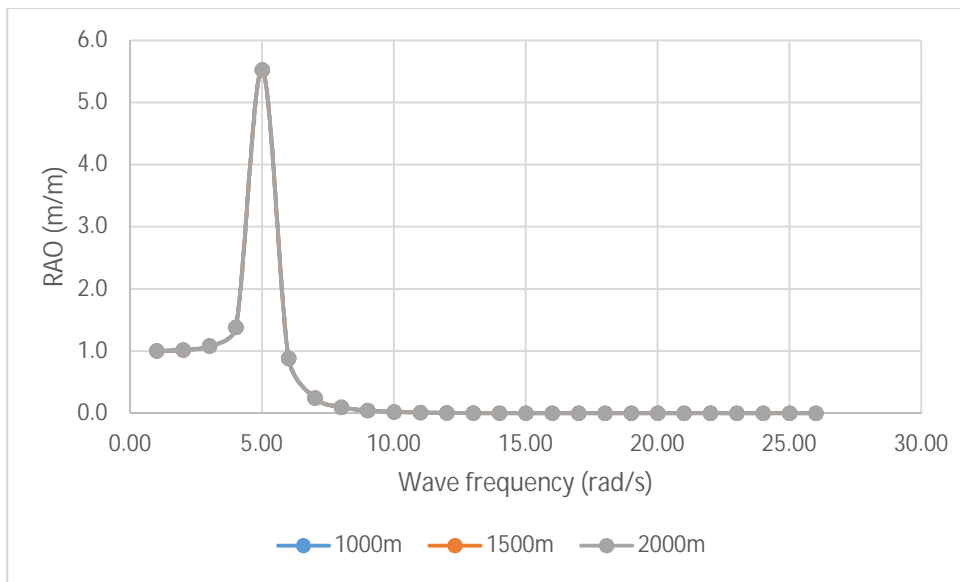


Figure 4.7: Spar heave RAO

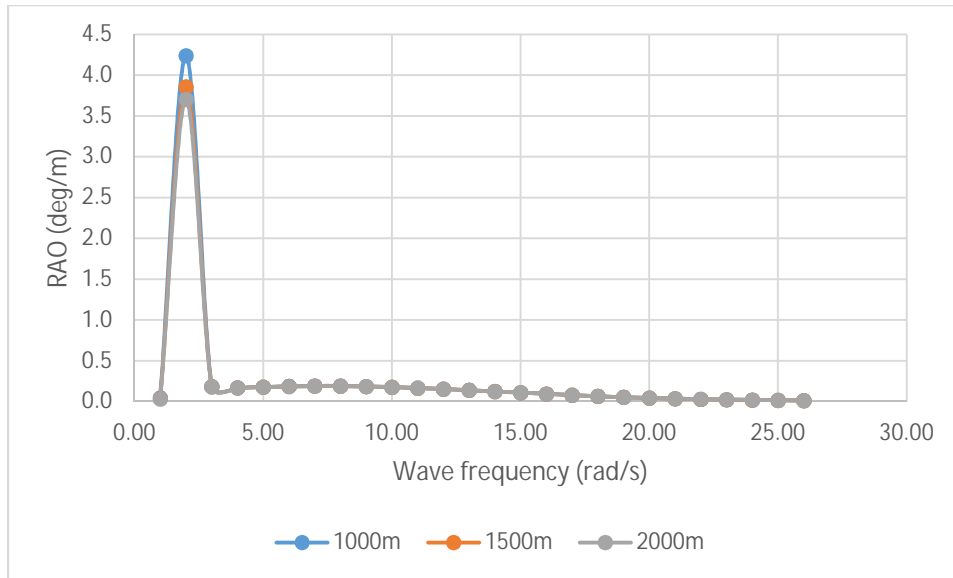


Figure 4.8: Spar pitch RAO

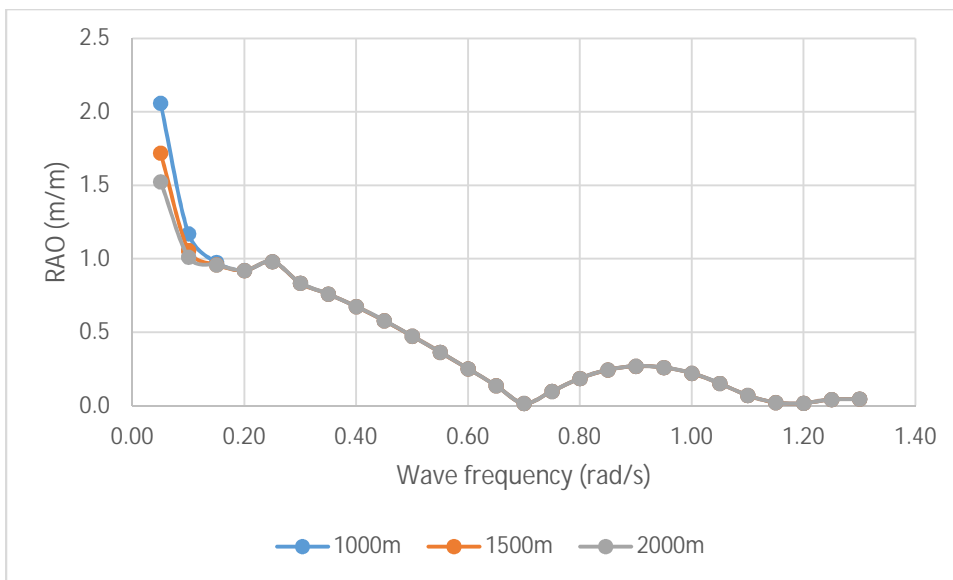


Figure 4.9: Semisubmersible surge RAO

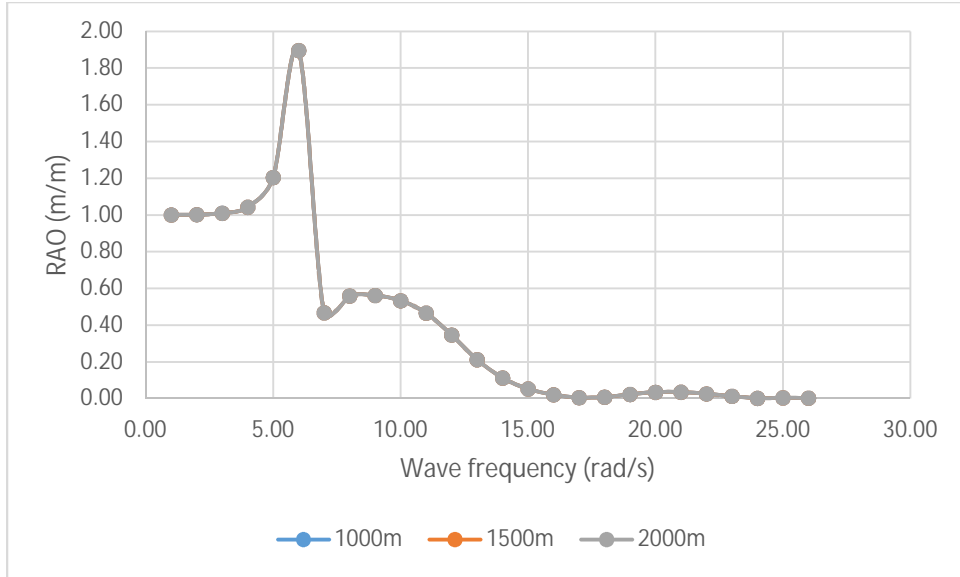


Figure 4.10: Semisubmersible heave RAO

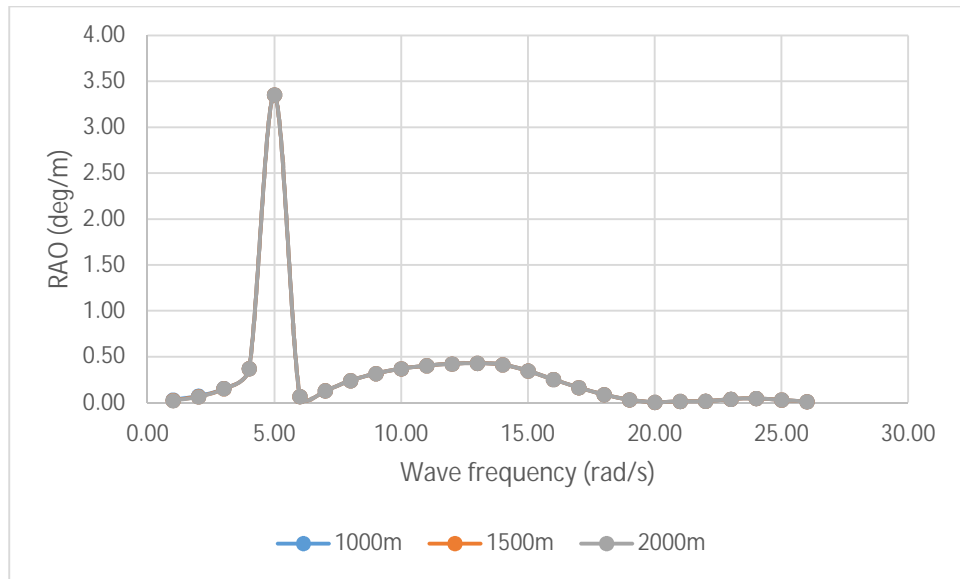


Figure 4.11: Semisubmersible pitch RAO

CHAPTER 5: CONCLUSION AND RECOMMENDATION

This study compared the dynamic responses of the spar and semisubmersible platforms under similar environment and cost-by-weight configuration. The primary element of wave is considered in the analysis. Several studies have been conducted to assess the hydrodynamic forces on the two platforms, but research is lacking to adequately compare the platforms under a similar cost factor. The spar and semisubmersible platform was modeled using HydroSTAR, which utilises the radiation/diffraction theory. Based on the findings, with the exception of the peak values, the spar's dynamic responses for the surge, heave and pitch are generally lower compared to the semisubmersible. At the water depth of 1000 m, the peak surge RAO for spar and semisubmersible has a negligible percentage difference of 0.005%; peak heave RAO for semisubmersible is 34% the value of the spar; and peak pitch RAO for semisubmersible is 79% the value of the spar. The surge response for the two platforms are relatively similar, having high RAO at low frequency, which generally decreases as the frequency increases. For the heave and pitch, the semisubmersible is found to achieve its peak RAO at a higher frequency compared to the spar. It was also noted that, after the sudden drop from peak, the semisubmersible's frequency increases slightly until a certain frequency before decreasing again. Concerning the spar however, after the peak points the responses for the majority gradually decreased with increasing frequency. Under increasing water depth, the surge response for the spar and semisubmersible decreases slightly at the low wave frequency. In addition, the peak pitch RAO for spar decreases slightly with increasing depth. The findings thus showed that overall, the spar performs better for the majority of the wave frequencies.

For further improvement, future studies should take into consideration the current and wind effect on the two platforms. In addition, research should be carried out to compare between alternative deepwater platforms such as the TLP and FPSO. These should be simulated under the same cost and environment as is currently carried out with the spar and semisubmersible, so that the platforms may be fairly assessed for their hydrodynamic performance.

REFERENCES

- Abbas, Y.M.E. (2011). *Studies On The Nonlinear Interactions Associated With Moored Semi Submersible Offshore Platforms*. PhD thesis, Universiti Teknologi PETRONAS.
- Chakrabarti, S. (2005). *Handbook of Offshore Engineering*. London: Elsevier.
- Chakrabarti, S.K. (2001). *Hydrodynamics of Offshore Structures*. Southampton: WIT Press.
- D'Souza, R., Aggarwal, R. & Basu, S. (2014). *A Comparison of Pre- and Post-2005 Sanctioned Gulf of Mexico Tension Leg, Semi-submersible and Spar Floating Platforms*. Offshore Technology Conference, Houston.
- Chen, X. (2002). *Studies on Dynamic Interaction between Deep-water Floating Structures and Their Mooring/Tendon Systems*. PhD dissertation, Texas A&M University.
- Hammett, D. S. (1983). Future Semi-Submersible Drilling Units. Society of Petroleum Engineers. doi:10.2118/11363-MS
- Kurian, V.J., Ng, C.Y. & Liew, M.S. (2012). Dynamic responses of classic spar platforms subjected to long crested waves: Morison equation vs. Diffraction theory. *Statistics in Science, Business, and Engineering (ICSSBE), 2012 International Conference*, pp.1-6. *Humanities, Science and Engineering (CHUSER), 2012 IEEE Colloquium on* , vol., no.,
- Kurian, V.J., Ng, C.Y. & Liew, M.S. (2012). Truss Spar Platform Motions for Combined Wave, Current and Wind Forces. *Business, Engineering & Industrial Applications Colloquium (BEIAC), 2012 IEEE Colloquium*.
- Kurian, V.J. and Ng, C.Y. and Liew, M. S. (2013). *Numerical and Experimental Study On Motion Responses Of Semi-Submersible Platforms Subjected To Short Crested Waves*. In: ICOVP2013 - International Conference on Vibration Problems, 9-12 Sep 2013, Lisbon.
- Latham, A. J. (2002). *Commercial Realities in Deep And Ultra Deepwater*. World Petroleum Congress.

Li, B., Liu, K., Yan, G. & Ou, J. (2011). *Hydrodynamic comparison of a semi-submersible, TLP, and Spar: Numerical study in the South China Sea environment*. Journal of Marine Science and Application. Volume 10, Issue 3, pp 306-314. Retrieved August 8, 2014, from <http://jmsaen.hrbeu.edu.cn/oa/pdffdown.aspx?Sid=20110308>

Liu, J., Yang, X., & Yu, H. (2010). *Heave And Pitch Motions of Floating Platform In South China Sea*. International Society of Offshore and Polar Engineers.

Ng, C.Y. (2010). *Dynamic Responses of Floating Offshore Platforms with Large Hulls*. Masters thesis, Civil Engineering Department, Universiti Teknologi PETRONAS.

Sablok, A. K. & Barras, S. A. (2009). *SS: Spar Technology - The Internationalization of the Spar Platform*. Offshore Technology Conference. doi:10.4043/20234-MS

Ye, W., Shanks, J., & Fang, J. (2003). *Effects of Fully Coupled and Quasi-Static Semi-Submersible Vessel Motions on Steel Catenary Riser's Wave Loading Fatigue*. Offshore Technology Conference. doi:10.4043/15105-MS

2. Kinematic boundary condition

$$\frac{\partial \eta}{\partial t} + \frac{\partial \Phi}{\partial x} \frac{\partial \eta}{\partial x} + \frac{\partial \Phi}{\partial z} \frac{\partial \eta}{\partial z} - \frac{\partial \Phi}{\partial y} = 0, \quad \text{on } y = \eta \quad (\text{A3})$$

Where:

$$u = \frac{\partial \Phi}{\partial x}, \quad v = \frac{\partial \Phi}{\partial y}, \quad w = \frac{\partial \Phi}{\partial z} \quad (\text{A4})$$

3. Bottom boundary condition

$$\frac{\partial \Phi}{\partial y} = 0, \quad \text{on } y = -d \quad (\text{A5})$$

4. Body surface boundary condition

$$\frac{\partial \Phi}{\partial \eta} = 0, \quad -d \leq y \leq \eta \quad (\text{A6})$$

The velocity potential (Φ) is the sum of the incident wave (Φ_0) and scattered velocity (Φ_s) potentials, expressed as

$$\Phi = \Phi_0 + \Phi_s \quad (\text{A7})$$

For Φ_s , the Sommerfeld radiation condition states that

$$\lim_{R \rightarrow \infty} \sqrt{R} \left(\frac{\partial}{\partial R} \pm i\lambda \right) \Phi_s = 0 \quad (\text{A8})$$

Where R = radial distance, $i = \sqrt{-1}$, and λ = eigenvalues.

Φ can assumed as a power series with respect to a perturbation parameter, ε

$$\Phi = \sum_{n=1}^{\infty} \varepsilon^n \Phi_n \quad (\text{A9})$$

In which ε is commonly chosen as

$$\varepsilon = \frac{kH}{2} \quad (\text{A10})$$

The free surface elevation η can also be written in series

$$\eta = \sum_{n=1}^{\infty} \varepsilon^n \eta_n \quad (\text{A11})$$

Where η_n = profile of the n^{th} order waves.

For the first and second order dynamic fluid pressures, p_1 and p_2 respectively are

$$p_1 = \rho \frac{\partial \Phi_1}{\partial t}; \quad p_2 = \rho \frac{\partial \Phi_2}{\partial t} + \frac{1}{2} \rho (\nabla \Phi_1)^2 \quad (\text{A12})$$

The force in a direction can then be represented as

$$F_{nj} = \varepsilon^n \iint_S p_n n_j dS \quad (\text{A13})$$

Where F_{nj} = the n^{th} order force in the direction, j , S = submerged profile and n_j = direction normal in the j direction of interest.

Raw data

SPAR

Wave frequency (rad/s)	SURGE			HEAVE			PITCH		
	Water depth			Water depth			Water depth		
	1000m	1500m	2000m	1000m	1500m	2000m	1000m	1500m	2000m
0.05	2.05E+00	1.71E+00	1.52E+00	1.00E+00	1.00E+00	1.00E+00	4.49E-02	3.76E-02	3.33E-02
0.10	6.41E-01	5.65E-01	5.35E-01	1.02E+00	1.02E+00	1.01E+00	4.24E+00	3.86E+00	3.70E+00
0.15	8.93E-01	8.78E-01	8.76E-01	1.08E+00	1.08E+00	1.08E+00	1.85E-01	1.82E-01	1.82E-01
0.20	8.13E-01	8.12E-01	8.12E-01	1.38E+00	1.38E+00	1.38E+00	1.69E-01	1.69E-01	1.69E-01
0.25	7.38E-01	7.38E-01	7.38E-01	5.52E+00	5.52E+00	5.52E+00	1.78E-01	1.78E-01	1.78E-01
0.30	6.60E-01	6.60E-01	6.60E-01	8.82E-01	8.82E-01	8.82E-01	1.87E-01	1.87E-01	1.87E-01
0.35	5.85E-01	5.85E-01	5.85E-01	2.44E-01	2.44E-01	2.44E-01	1.91E-01	1.91E-01	1.91E-01
0.40	5.15E-01	5.15E-01	5.15E-01	9.63E-02	9.63E-02	9.63E-02	1.90E-01	1.90E-01	1.90E-01
0.45	4.51E-01	4.51E-01	4.51E-01	4.31E-02	4.31E-02	4.31E-02	1.85E-01	1.85E-01	1.85E-01
0.50	3.92E-01	3.92E-01	3.92E-01	2.06E-02	2.06E-02	2.06E-02	1.76E-01	1.76E-01	1.76E-01
0.55	3.40E-01	3.40E-01	3.40E-01	1.02E-02	1.02E-02	1.02E-02	1.66E-01	1.66E-01	1.66E-01
0.60	2.93E-01	2.93E-01	2.93E-01	5.12E-03	5.12E-03	5.12E-03	1.53E-01	1.53E-01	1.53E-01
0.65	2.50E-01	2.50E-01	2.50E-01	2.57E-03	2.57E-03	2.57E-03	1.39E-01	1.39E-01	1.39E-01
0.70	2.11E-01	2.11E-01	2.11E-01	1.28E-03	1.27E-03	1.27E-03	1.24E-01	1.24E-01	1.24E-01
0.75	1.76E-01	1.76E-01	1.76E-01	6.24E-04	6.24E-04	6.24E-04	1.09E-01	1.09E-01	1.09E-01
0.80	1.44E-01	1.44E-01	1.44E-01	3.04E-04	3.03E-04	3.04E-04	9.35E-02	9.35E-02	9.35E-02
0.85	1.17E-01	1.17E-01	1.17E-01	1.52E-04	1.52E-04	1.52E-04	7.87E-02	7.87E-02	7.87E-02
0.90	9.36E-02	9.36E-02	9.36E-02	8.49E-05	8.49E-05	8.49E-05	6.53E-02	6.53E-02	6.53E-02
0.95	7.45E-02	7.45E-02	7.45E-02	5.68E-05	5.68E-05	5.68E-05	5.36E-02	5.36E-02	5.36E-02
1.00	5.91E-02	5.91E-02	5.91E-02	4.47E-05	4.47E-05	4.46E-05	4.36E-02	4.36E-02	4.36E-02
1.05	4.69E-02	4.69E-02	4.69E-02	3.81E-05	3.81E-05	3.84E-05	3.54E-02	3.54E-02	3.54E-02
1.10	3.73E-02	3.73E-02	3.73E-02	3.39E-05	3.39E-05	3.44E-05	2.87E-02	2.87E-02	2.87E-02
1.15	2.98E-02	2.98E-02	2.98E-02	3.03E-05	3.01E-05	3.07E-05	2.33E-02	2.33E-02	2.33E-02
1.20	2.39E-02	2.39E-02	2.39E-02	2.70E-05	2.74E-05	2.72E-05	1.90E-02	1.90E-02	1.90E-02
1.25	1.93E-02	1.93E-02	1.93E-02	2.40E-05	2.45E-05	2.40E-05	1.55E-02	1.55E-02	1.55E-02
1.30	1.57E-02	1.57E-02	1.57E-02	2.05E-05	2.09E-05	2.03E-05	1.28E-02	1.28E-02	1.28E-02

SEMISUBMERSIBLE

Wave frequency (rad/s)	Surge RAO (m/m)			Heave RAO (m/m)			Pitch RAO (m/m)		
	Water depth			Water depth			Water depth		
	1000m	1500m	2000m	1000m	1500m	2000m	1000m	1500m	2000m
0.05	2.06E+00	1.72E+00	1.52E+00	1.00E+00	1.00E+00	1.00E+00	3.05E-02	2.55E-02	2.26E-02
0.10	1.17E+00	1.06E+00	1.01E+00	1.00E+00	1.00E+00	1.00E+00	7.33E-02	6.62E-02	6.33E-02
0.15	9.76E-01	9.60E-01	9.58E-01	1.01E+00	1.01E+00	1.01E+00	1.56E-01	1.53E-01	1.53E-01
0.20	9.21E-01	9.21E-01	9.21E-01	1.04E+00	1.04E+00	1.04E+00	3.71E-01	3.71E-01	3.71E-01
0.25	9.81E-01	9.81E-01	9.81E-01	1.20E+00	1.20E+00	1.20E+00	3.35E+00	3.35E+00	3.35E+00
0.30	8.35E-01	8.35E-01	8.35E-01	1.90E+00	1.90E+00	1.90E+00	6.77E-02	6.77E-02	6.77E-02
0.35	7.60E-01	7.60E-01	7.60E-01	4.68E-01	4.68E-01	4.68E-01	1.31E-01	1.31E-01	1.31E-01
0.40	6.75E-01	6.75E-01	6.75E-01	5.59E-01	5.59E-01	5.59E-01	2.40E-01	2.40E-01	2.40E-01
0.45	5.79E-01	5.79E-01	5.79E-01	5.62E-01	5.62E-01	5.62E-01	3.17E-01	3.17E-01	3.17E-01
0.50	4.74E-01	4.74E-01	4.74E-01	5.33E-01	5.33E-01	5.33E-01	3.70E-01	3.70E-01	3.70E-01
0.55	3.64E-01	3.64E-01	3.64E-01	4.66E-01	4.66E-01	4.66E-01	4.04E-01	4.04E-01	4.04E-01
0.60	2.52E-01	2.52E-01	2.52E-01	3.46E-01	3.46E-01	3.46E-01	4.22E-01	4.22E-01	4.22E-01
0.65	1.37E-01	1.37E-01	1.37E-01	2.12E-01	2.12E-01	2.12E-01	4.30E-01	4.30E-01	4.30E-01
0.70	1.63E-02	1.63E-02	1.63E-02	1.12E-01	1.12E-01	1.12E-01	4.14E-01	4.14E-01	4.14E-01
0.75	9.77E-02	9.77E-02	9.77E-02	5.27E-02	5.27E-02	5.27E-02	3.47E-01	3.47E-01	3.47E-01
0.80	1.86E-01	1.86E-01	1.86E-01	2.10E-02	2.10E-02	2.10E-02	2.53E-01	2.53E-01	2.53E-01
0.85	2.44E-01	2.44E-01	2.44E-01	5.27E-03	5.27E-03	5.27E-03	1.65E-01	1.65E-01	1.65E-01
0.90	2.69E-01	2.69E-01	2.69E-01	7.89E-03	7.89E-03	7.89E-03	8.87E-02	8.87E-02	8.87E-02
0.95	2.60E-01	2.60E-01	2.60E-01	2.31E-02	2.31E-02	2.31E-02	3.18E-02	3.18E-02	3.18E-02
1.00	2.21E-01	2.21E-01	2.21E-01	3.46E-02	3.46E-02	3.46E-02	4.93E-03	4.93E-03	4.93E-03
1.05	1.52E-01	1.52E-01	1.52E-01	3.51E-02	3.51E-02	3.51E-02	1.53E-02	1.53E-02	1.53E-02
1.10	7.06E-02	7.06E-02	7.06E-02	2.58E-02	2.58E-02	2.58E-02	1.69E-02	1.69E-02	1.69E-02
1.15	2.18E-02	2.18E-02	2.18E-02	1.29E-02	1.29E-02	1.29E-02	3.83E-02	3.83E-02	3.83E-02
1.20	1.72E-02	1.72E-02	1.72E-02	1.56E-03	1.56E-03	1.56E-03	4.71E-02	4.71E-02	4.71E-02
1.25	4.25E-02	4.25E-02	4.25E-02	4.35E-03	4.35E-03	4.35E-03	3.05E-02	3.05E-02	3.05E-02
1.30	4.61E-02	4.61E-02	4.61E-02	2.44E-03	2.44E-03	2.44E-03	1.16E-02	1.16E-02	1.16E-02